Molecular Microbiology (2008) 68(1), 110–123 ■
doi:10.1111/j.1365-2958.2008.06141.x
First published online 26 February 2008

Structural and mutational analysis of the cell division protein FtsQ

Fusinita van den Ent,[1]* Thessa M. F. Vinkenvleugel,[2] Alice Ind,[1] Philip West,[1] Dmitry Veprintsev,[1] Nanne Nanninga,[2] Tanneke den Blaauwen[2] and Jan Löwe[1]

[1]*MRC-LMB, Hills Road, Cambridge CB2 2QH, UK.*
[2]*Swammerdam Institute for Life Sciences, Molecular Cytology, Kruislaan 316, 1098 SM Amsterdam, the Netherlands.*

Summary

Bacterial cytokinesis requires the divisome, a complex of proteins that co-ordinates the invagination of the cytoplasmic membrane, inward growth of the peptidoglycan layer and the outer membrane. Assembly of the cell division proteins is tightly regulated and the order of appearance at the future division site is well organized. FtsQ is a highly conserved component of the divisome among bacteria that have a cell wall, where it plays a central role in the assembly of early and late cell division proteins. Here, we describe the crystal structure of the major, periplasmic domain of FtsQ from *Escherichia coli* and *Yersinia enterocolitica*. The crystal structure reveals two domains; the α-domain has a striking similarity to polypeptide transport-associated (POTRA) domains and the C-terminal β-domain forms an extended β-sheet overlaid by two, slightly curved α-helices. Mutagenesis experiments demonstrate that two functions of FtsQ, localization and recruitment, occur in two separate domains. Proteins that localize FtsQ need the second β-strand of the POTRA domain and those that are recruited by FtsQ, like FtsL/FtsB, require the surface formed by the tip of the last α-helix and the two C-terminal β-strands. Both domains act together to accomplish the role of FtsQ in linking upstream and downstream cell division proteins within the divisome.

Introduction

Cytokinesis in bacteria requires a complex of proteins, called the divisome that forms a septal ring at the future division site. The divisome regulates constriction of the cell envelope, it synchronizes membrane fusion and scission and co-ordinates septal peptidoglycan synthesis (Goehring and Beckwith, 2005; Vicente and Rico, 2006). In *Escherichia coli*, at least 12 proteins play an essential role in this process, FtsZ, FtsA, ZipA, FtsE, FtsX, FtsK, FtsQ, FtsB, FtsL, FtsW, PBP3 (FtsI) and FtsN. They localize to a ring-like structure at midcell together with the non-essential proteins PBP1B, AmiC, EnvC, Tol and Pal (Bernhardt and de Boer, 2003; Bernhardt and de Boer, 2004; Bertsche *et al.*, 2006; Gerding *et al.*, 2007). Mutants that stop dividing and grow as filamentous cells indicate the importance of these proteins for cell division.

The cytoplasmic, tubulin-like protein FtsZ (Mukherjee *et al.*, 1993; Erickson, 1995; Löwe and Amos, 1998) is first to localize at the future division site. The GTPase activity as well as its polymerisation capacity might provide the force necessary to constrict the cell (de Boer *et al.*, 1992; RayChaudhuri and Park, 1992; Mukherjee and Lutkenhaus, 1994; Erickson *et al.*, 1996; Yu and Margolin, 1997; Löwe and Amos, 1999; Lu *et al.*, 2000). FtsZ forms a ring-like structure at midcell, where it is stabilized by the cytoplasmic proteins FtsA and ZapA as well as the inner membrane protein ZipA (Pichoff and Lutkenhaus, 2002; 2005). In *E. coli*, these early division proteins assemble at midcell prior to the recruitment of the other divisome components that localize in a hierarchical manner (FtsE < FtsX < FtsK < FtsQ < FtsL/FtsB < FtsW < FtsI < FtsN < AmiC) (Chen and Beckwith, 2001; Aarsman *et al.*, 2005).

Despite the sequential dependency in which the cell division proteins seem to localize, some of the components of the divisome can form a complex before they reach the septum independent of their usual recruitment partner, making a purely linear assembly pathway unlikely (Buddelmeijer and Beckwith, 2004; Goehring *et al.*, 2005; 2006; Vicente and Rico, 2006). The localization dependency of FtsQ on the presence of the early division proteins can be bypassed by fusing FtsQ to ZapA (Goehring *et al.*, 2005). The fusion can back-recruit FtsK supporting a direct interaction between FtsQ and FtsK *in vivo* (Goehring *et al.*, 2005). Also, it has been shown that FtsQ can form a sub-complex with FtsL and FtsB away from the division site and independent of FtsK, which is required for its localization (Buddelmeijer and Beckwith, 2004).

Accepted 23 January, 2008. *For correspondence. E-mail fent@mrc-lmb.cam.ac.uk; Tel. (+44) 1223 252969; Fax (+44) 1223 213556.

Complex formation is probably important for the stabilizing effect of FtsQ on FtsL (Daniel and Errington, 2000) and the requirement of FtsQ for the recruitment of FsL/FtsB to the divisome (Weiss *et al*., 1999). The hypothesis that FtsQ might be involved in maintaining FtsL's stability comes from work in *Bacillus subtilis*. In *Bacillus*, the FtsQ homologue Div1B is only essential at elevated temperatures (Errington *et al*., 2003), whereas the temperature dependence of certain mutants in Div1B can be overcome by the overexpression of FtsL. Therefore, FtsQ might regulate the stoichiometry of the FtsL/FtsB sub-complex by stabilizing FtsL.

In *E. coli*, FtsQ is present in approximately 25–50 copies per cell (Carson *et al*., 1991), where it has a central role in the formation of the divisome. FtsQ is a bitopic membrane protein of 31 kDa (Robinson *et al*., 1984), consisting of a short cytoplasmic tail (residues 1–24), a transmembrane region (25–49) and a periplasmic domain of approximately 226 residues (Carson *et al*., 1991; Guzman *et al*., 1997). Previously, it has been suggested that the periplasmic domain can be divided into three domains (Robson and King, 2006). Based on the primary sequence, Sánchez-Pulido *et al*., (2003) predicted that the first domain would resemble a POTRA (polypeptide transport-associated) domain. POTRA domains are usually involved in chaperone-like functions, but whether that is the case for FtsQ remains to be established. An nuclear magnetic resonance (NMR) structure is available of 119 residues of the periplasmic region of DivIB from *Geobacillus stearothermophilus*, which comprises the second domain (Robson and King, 2006). According to the authors, the second domain adopts two conformations that might be involved in modulating protein–protein interactions in the flanking domains. The third domain would be unstructured in the absence of other cell division proteins.

The central role of FtsQ in the divisome becomes apparent from the number of interaction partners it can bind to; two-hybrid analyses suggest a highly interconnected network of proteins, where FtsQ interacts with FtsA, FtsK, FtsX, FtsL, FtsB, FtsW, FtsI, FtsN and YmgF (Di Lallo *et al*., 2003; Karimova *et al*., 2005; D'Ulisse *et al*., 2007). Some of the interactions found in two-hybrid assays were confirmed by co-immunoprecipitation, such as those between FtsL, FtsB and FtsQ (Buddelmeijer and Beckwith, 2004), between FtsQ and FtsW or between FtsN, FtsI and FtsK (D'Ulisse *et al*., 2007). The early cell division proteins FtsA and FtsK bind to the cytoplasmic tail of FtsQ, whereas all the other interactions depend on the periplasmic domain and/or the transmembrane region (Di Lallo *et al*., 2003; Karimova *et al*., 2005; D'Ulisse *et al*., 2007). Domain swap experiments also indicate the importance of the periplasmic part of FtsQ for its localization as well as for the recruitment of downstream proteins (Guzman *et al*., 1997; Buddelmeijer *et al*., 1998; Chen *et al*., 1999).

Despite being discovered over 25 years ago, the exact role of FtsQ remains unknown. Overproduction of FtsQ causes filamentation (Carson *et al*., 1991), suggesting that the level of FtsQ needs to be tightly controlled for optimal cell division. From the *in vivo* interaction studies described above, it becomes clear that FtsQ links cytoplasmic and periplasmic cell division proteins and might, indirectly, affect peptidoglycan synthesis (Piette *et al*., 2004). The role of FtsQ in cell wall synthesis is supported by the high abundance of the FtsQ homologue DivIB in *B. subtilis* [5000 molecules per cell (Rowland *et al*., 1997), versus 25–50 in *E. coli* (Carson *et al*., 1991)], which might reflect the need to build a thicker cell wall in *B. subtilis* (Katis and Wake, 1999). In addition, FtsQ only occurs in bacteria that possess a cell wall (Alarcon *et al*., 2007) and has some, although low sequence similarity to the peptidoglycan recycling factor Mpl (Mengin-Lecreulx *et al*., 1996). However, no experimental proof for a direct role of FtsQ in cell wall synthesis has been obtained so far.

Here, we describe the crystal structure of the major, periplasmic domain of FtsQ from *E. coli* and *Yersinia enterocolitica*. The structure reveals two domains. The α-domain is strikingly similar to POTRA domains, whereas the C-terminal β-domain forms an extended β-sheet overlaid by two slightly bent α-helices. Although the crystal structure depicts a dimer, analytical ultracentrifugation analyses of the periplasmic region of FtsQ from five different species indicate that the majority of the protein is monomeric. Point mutations in the POTRA domain of FtsQ were identified that affect FtsQ localization and mutations in the C-terminal region of the second domain, previously called the γ-domain, hamper the recruitment of downstream binding partners. These results highlight specific regions in the structure of FtsQ required for the role of FtsQ in linking upstream and downstream cell division proteins within the divisome.

Results and discussion

Crystal structure FtsQ

The crystal structure of the major, periplasmic domain of FtsQ from the Gram-negative bacteria *E. coli* and *Y. enterocolitica* reveals an elongated, slightly bent molecule consisting of two domains (Fig. 1). The smaller domain (coloured in red in Fig. 1) is located close to the membrane and encompasses a three-stranded β-sheet on top of which are two anti-parallel α-helices. The topology of the α-domain is β-α-α-β-β, where the third β-strand is packed in between the first and the second strands. The C-terminal, larger domain (green in Fig. 1) is composed of a slightly bent β-sheet, consisting of nine β-strands, overlaid on the convex side by two long α-helices. Following the α-domain, three short anti-parallel β-strands precede a

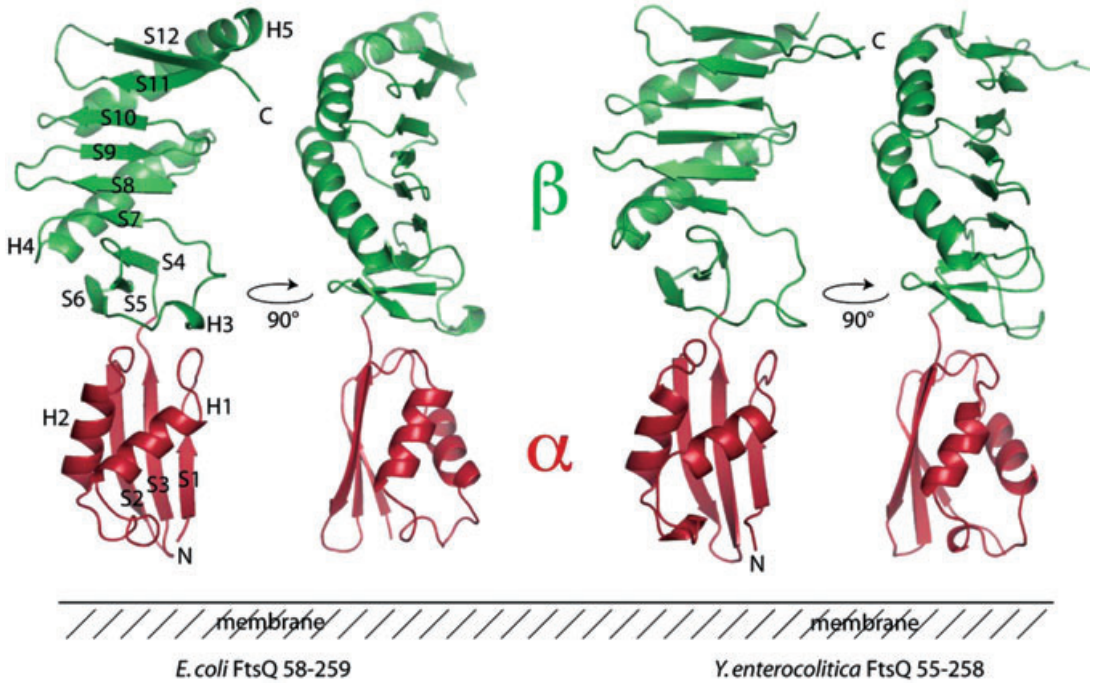

Fig. 1. Ribbon plot of the crystal structure of the major periplasmic part of FtsQ (aa 58–260) from *E. coli* (left). The secondary structure elements are labelled according to their appearance in the primary sequence. A 90° rotation along the *y*-axis of the *E. coli* FtsQ structure shows the curved nature of the second domain. On the right, ribbon plot of *Y. enterocolitica* FtsQ periplasmic domain (residues 55–258) and its 90° rotation along the *y*-axis. The sequences of *E. coli* and *Y. enterocolitica* FtsQ are 56% identical and both structures superimpose with an rmsd of 1.63 Å (Z-score 7.1). Figures were prepared using PYMOL.

helical loop, which runs into β-strand S7. The parallel β-strands S7 and S8 are linked by helix H4. Strands S9 and S10 pack against S8 in an anti-parallel fashion and are connected to the remaining β-strands S11 and S12 via a slightly kinked α-helix (H5). The C-terminal 15 residues of FtsQ are disordered in the crystal structure, which have been shown to be dispensable for FtsQ function (Goehring *et al.*, 2007). *E. coli* and *Y. enterocolitica* FtsQ share 56% of their sequence, enough to ensure a similar fold as the structures superimpose with their C_α atoms with a root mean square deviation (rmsd) of 1.63 Å (Fig. 1). Both crystal structures contain a dimer in the asymmetric unit. In the case of *E. coli* FtsQ, the monomer dimerizes tail-to-tail, with the C-terminal β-strand S12 and α-helix H5. As the angle between the monomers is almost 180°, the overall shape of the asymetric unit is long and thin, accounting for the anisotropic diffraction observed for *E. coli* FtsQ (Fig. 2). The dimeric interface buries 882 $Å^2$ of solvent accessible surface for each monomer, which implies that additional contacts might be needed to ensure dimer formation *in vivo*

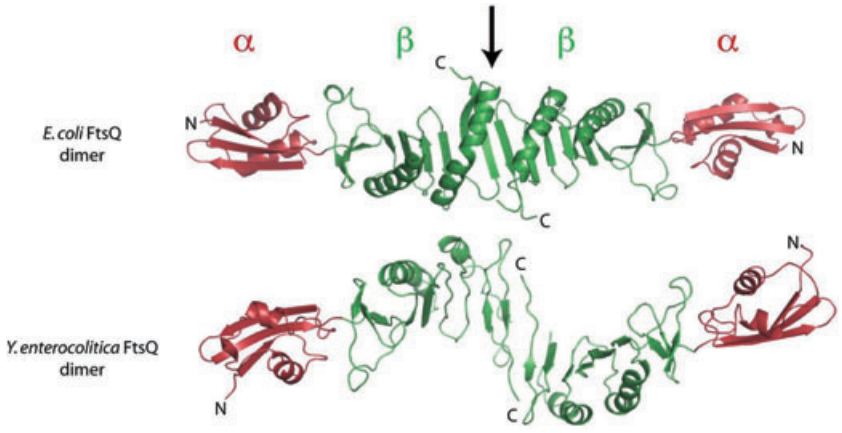

Fig. 2. A. Ribbon plot of the dimer observed in the crystals of *E. coli* FtsQ. The dimer of *E. coli* FtsQ forms a curved, elongated β-sheet composed of 18 β-strands. The arrow points to the dimer interface.
B. In the crystals *Y. enterocolitica* FtsQ is arranged in a similar way.

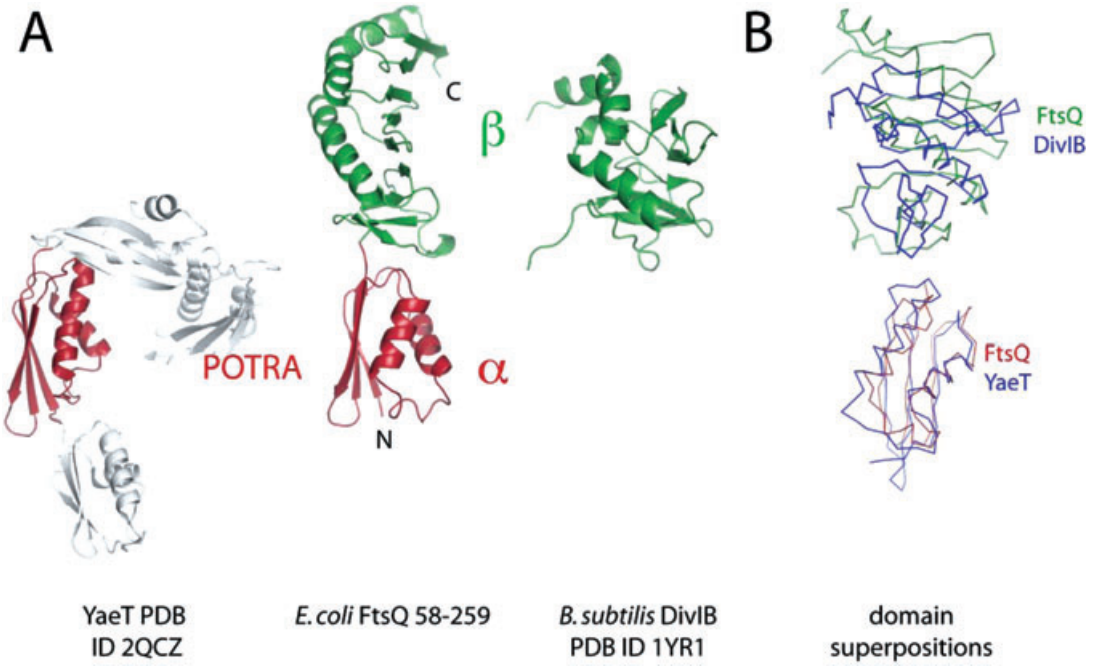

Fig. 3. A. Structural similarity between the α-domain of the periplasmic part of FtsQ (shown in red) and the POTRA domain P2 of YaeT, which superimpose with an rmsd of 1.8 Å (Z-score 8.1) [DALI (Holm and Sander, 1993)]. The second domain of FtsQ (depicted in green) superimposes on the β-domain of DivIB from *G. stearothermophilus* with an rmsd of 3.9 Å (Z-score 4.1).
B. Top: superposition of the β-domain of *E. coli* FtsQ (green) on the β-domain of DivIB from *G. stearothermophilus* (blue). Bottom: superposition of the α-domain of *E. coli* FtsQ (red) on the POTRA domain (blue). The figure was prepared using PYMOL.

(see below). The monomers in the asymmetric unit of *Y. enterocolitica* FtsQ arrange in a head-to-tail fashion, with an angle of about 45° between the monomers. However, in the crystals, a similar contact as observed for *E. coli* FtsQ does exist, where both of the C-terminal β-strands (S12) are involved in protein–protein interaction between molecules belonging to different asymmetric units. This suggests that the surface exposed by the C-terminal β-strand is prone to protein–protein interaction, whether this is dimer formation or interaction with a different protein will be discussed below.

A similarity search among the currently known structures in the protein databank with DALI (Holm and Sander, 1993) reveals a striking similarity between the α-domain of FtsQ and the POTRA domain P2 of YaeT from *E. coli* (Fig. 3). YaeT is an integral, outer membrane protein with a periplasmic region consisting of five POTRA domains of which homologues have been found in mitochondria (Sam50) and chloroplasts (Toc75). The POTRA domains of YaeT are involved in folding integral β-barrel proteins. As described for the α-domain of FtsQ, the first and second strands of the POTRA domain form the edges of a three-stranded β-sheet, with the third strand packed between them. It has been proposed that some of the exposed edges of the POTRA domains might assist in the assembly of β-barrels of outer membrane proteins via β-strand augmentation (Harrison, 1996). This would allow POTRA domains to interact with many different proteins, as long as they provide the necessary hydrophobic periodicity (Kim *et al*., 2007). The N-terminal 60 residues of the periplasmic part of FtsQ superimpose on the second POTRA domain of YaeT with an rmsd of 1.8 Å (Z-score is 8.1) and share the hydrophobic residues that built up the core of the structure. The regular appearance of these hydrophobic residues was the reason for Sánchez-Pulido *et al*. (2003) to predict this region would adopt a POTRA domain-like fold, which the crystal structure confirms. It has been suggested that this domain might be involved in a chaperone-like activity stabilizing FtsL (Sánchez-Pulido *et al*., 2003; Robson and King, 2006). However, mutations affecting the interaction between FtsL and FtsQ map to the C-terminus of FtsQ (see below) and the POTRA domain might interact with other FtsQ localizing factors.

The C-terminus of FtsQ superimposes on DivIB from *G. stearothermophilus* with an rmsd of 3.9 Å (Z-score is 4.1, with 86 residues). Although the sequence identity is low (19%), it has generally been accepted that DivIB is the FtsQ homologue in Gram-positive bacteria because of its size, its location in the genome and its role in cell division. In addition, the growth of *E. coli* bacterial strains depleted for FtsQ is partially complemented by *Streptococcus pneumoniae* DivIB (D'Ulisse *et al*., 2007). Both structures

superimpose quite well along the β-sheet between S6 and S10 as well as Helix H4, with the exception of strand S4 (Fig. 3). In the crystal structure, S4 is connected to the POTRA domain and adopts a slightly tighter angle than in the NMR structure, where it is at the start of the expressed construct. The other discrepancy between the NMR and the crystal structure is the C-terminal α-helix H5. In the crystal structure, this helix is continuous, whereas in the NMR structure the helix breaks at Pro222 (see structural alignment in supplementary information), adopting either one of two conformations that have their C-termini pointing into opposite directions. This proline is not highly conserved among FtsQ or DivIB homologues, but it is present in *E. coli* FtsQ, where it induces a slight kink in the helix. The helix is stabilized by the last two β-strands of FtsQ that built on the large, C-terminal β-sheet. The construct used for the NMR study was a truncated version, excluding the last two β-strands, which might have been the reason that the helix adopted two different conformations.

Based on proteolysis experiments, Robson and King (2006) proposed that DivIB would have a third domain (γ), encompassing the last two β-strands that would only be stabilized upon interaction with other cell division proteins. As shown in Fig. 1, this region in both *E. coli* and *Y. enterocolitica* FtsQ is well ordered in the absence of other cell division proteins and is part of the extended β-sheet of the second domain. Also, the majority of the 50 constructs we tried to crystallize were stably expressed as full-length periplasmic versions, which makes it rather unlikely that the γ-domain is a separate entity. Therefore, the appearance of the γ-domain after proteolytic treatment of the protein is a sign of the presence of a flexible loop between helix H5 and strand S11, rather than an indication of a separate domain.

Is FtsQ a monomer or a dimer?

Contradicting results have been reported on the oligomeric state of FtsQ. Bacterial two-hybrid experiments agree on FtsQ dimerization, although the region required for dimerization is different in different reports; Karimova *et al*. (2005) suggest that dimerization is abolished upon truncation of the C-terminal 30 residues, whereas D'Ulisse *et al*. (2007) indicated that FtsQ is able to self-interact as long as the transmembrane region and the cytoplasmic tail are present, both by two-hybrid analysis and by co-immune precipitation. In contrast, other co-immune precipitation experiments have shown that FtsQ does not form homodimers (Goehring *et al*., 2006), which was confirmed by multi-angle laser scattering with the purified, periplasmic region of *G. stearothermophilus* DivIB (Robson and King, 2006).

Our analytical ultracentrifugation of the periplasmic region of *E. coli* FtsQ shows that the protein is monomeric

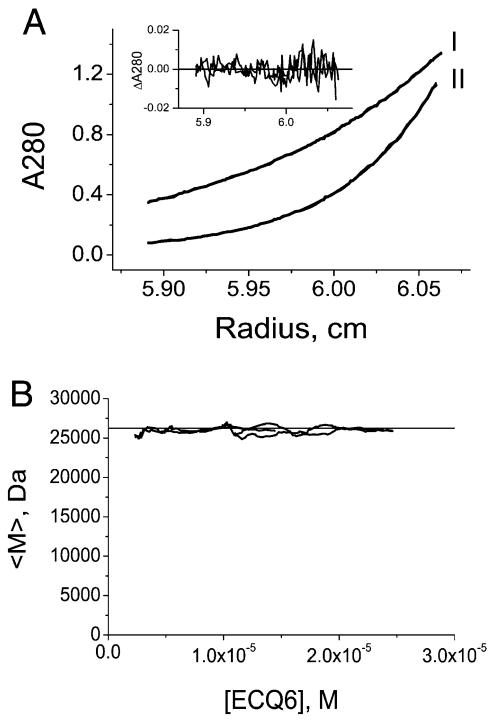

Fig. 4. Analytical ultracentrifugation. The periplasmic part of *E. coli* FtsQ was subjected to a sedimentation equilibrium run at a concentration of 26 μM.
A. The absorption at 280 nm was plotted against the radius (cm) of the cell at a speed of 20 k.r.p.m. (marked I) and 30 k.r.p.m. (marked II). The inset shows the residuals of both runs fitted as a single species (monomer).
B. The calculated mass was plotted against the concentration of the protein, and the molecular mass remains that from a monomer with increasing the concentration of the protein to 25 μM.

at a concentration of 26 μM (Fig. 4). The calculated mass is 25.9 kDa (±0.1 kDa), close to the expected mass of 26.2 kDa. The equilibrium runs of the periplasmic part of FtsQ from *Y. enterocolitica*, *Staphylococcus aureus*, *Corynebacterium diphtheria* and *Listeria monocytogenes* were run at a similar concentration and confirmed that the majority of the protein is monomeric. As these experiments were done with the major, periplasmic region of FtsQ, we cannot exclude the effect the transmembrane segment might have on the oligomerization state of FtsQ *in vivo*, which might enhance the local concentration and promote oligomerization.

Mutational analysis of FtsQ

The first evidence that the two functions of FtsQ, localization and recruitment, are genetically separable came from a C-terminal deletion mutant, *ftsQ2*, which localized normally, but failed to recruit downstream proteins (Chen *et al*., 2002). To dissect the regions of FtsQ that are required for different functions further, we examined the effect of introducing point mutations on either FtsQ

localization or recruitment of downstream proteins and mapped them onto the structure.

FtsQ localization

Mutants that affect the localization of FtsQ could indicate regions in FtsQ that are required for interaction with upstream proteins that localize FtsQ, such as FtsK. As shown in Fig. 5B, replacing the conserved K113 with an aspartic acid in *E. coli* FtsQ impairs FtsQ localization, whereas mutating the semi-conserved D91 with either lysine (Fig. 5C) or a glutamine (data not shown) does not have such an effect. Mutant proteins were expressed as green fluorescent protein (GFP)-fusions and, although the levels of expression were slightly reduced compared with wild-type (WT) GFP–FtsQ, the proteins were intact (Fig. 5H). As D91 is pointing outwards into the solvent and consequently does not affect the structural integrity of the protein, it is reasonable to assume that upstream proteins do not require D91 for FtsQ localization. Lysine 113 is part of the second β-strand and is in contact with the main chain oxygen of residues M88 and Q90. Introducing an aspartic acid at this position might displace the second β-strand, suggesting that the α-domain of FtsQ might be involved in the interaction of upstream cell division proteins that are responsible for its localization. To investigate this further, the effect of additional mutations was examined. Mutation of the conserved glutamic acid 125 to lysine eliminated localization to midcell at the restrictive temperature (Taschner *et al*., 1988; Aarsman *et al*., 2005). The high degree of conservation of E125 is most likely for structural reasons. It is located at the opposite end of the α-domain, close to tip of the third β-strand, where its side-chain interacts with the main-chain nitrogen of residues Y68 and H69. Introducing a positively charged lysine residue at this position will disrupt the interaction and most likely affect the fold of the α-domain. Although both K113 and E125 are located on opposite sides of the α-domain, they have a similar phenotype and are unable to complement each other (Fig. 5F).

Other mutants of FtsQ that fail to localize are *ftsQ6* carrying mutations F145L and L181R and *ftsQ15* that has three residues replaced: Q108L, V111G, Y227D (Chen *et al*., 2002). The synergistic effect of combinations of mutations in both *ftsQ6* and *ftsQ15* is needed to impede septal targeting. Both mutated residues of FtsQ6 are widely separated in the C-terminal domain and have their side-chains pointing into the hydrophobic core. Mutations of these residues will most likely unfold the protein, making it difficult to assess the importance of these residues for localization. The triple mutant FtsQ15 has two of its mutations located in the α-domain (Q108L and V111G) and the third in the C-terminal helix H5 (Y227D). Again, the latter being part of the hydrophobic core of the C-terminal domain is a structural mutant. However, Q108, located in second β-strand, is solvent exposed. Also V111, although instrumental for the formation of the hydrophobic core between β-strand S2 and α-helix H2, is accessible from the outside. This makes it highly likely that these residues are involved in an interaction with a protein that enables septal targeting of FtsQ.

Two more point mutations, L60P and V92D, hamper FtsQ localization (Goehring *et al*., 2007). As the solvent exposed L60 was replaced with a proline that might have affected the structural integrity of the first β-strand, the role of L60 in FtsQ localization is non-conclusive. However, V92 at the bottom of the second α-helix interacts with V111 and K113, establishing a hydrophobic contact between α-helix H2 and β-strand S2. In addition, all three amino acids are solvent accessible (Fig. 6).

Taken together, we propose that the residues that affect FtsQ localization without impeding the structural integrity of the protein, are V92, Q108, V111 and K113. They are part of the solvent exposed surface formed by the second β-strand and the tip of the second α-helix in the α-domain (Fig. 6). As these residues are relatively close to the membrane, it is feasible that they might interact with an extracellular loop of FtsK that is required for FtsQ localization.

Downstream interactions

As mentioned in the *Introduction*, bacterial two-hybrid data suggest that the periplasmic part of FtsQ is involved in the recruitment of downstream partners such as FtsL, FtsI and FtsN (Di Lallo *et al*., 2003; Karimova *et al*., 2005; D'Ulisse *et al*., 2007). The interaction between FtsQ and FtsN is genetically supported by the finding that overexpression of FtsN can partially suppress FtsQ1(ts) (Dai *et al*., 1993). However, there is no evidence for a direct interaction between the two proteins *in vitro*. Although the final crystals of *E. coli* FtsQ were obtained by mixing the protein with the structured part of the periplasmic domain of FtsN (see *Experimental procedures*), no interaction was observed between the two proteins in either size-exclusion chromatography or isothermal titration calorimetry (data not shown). It remains to be determined whether the purified, full-length proteins can establish a stable interaction *in vitro*. The transmembrane regions of cell division proteins complicate interaction studies, but it is possible and quite likely that these regions might facilitate interactions between some of the cell division proteins, such as FtsQ and FtsN.

Mutagenesis was performed to investigate which part of the periplasmic region of FtsQ is involved in the recruitment of the FtsL/FtsB complex. As shown in Fig. 5, WT FtsQ expressed together with sYFP1-FtsL in LMC531 cells (that contain the endogenous temperature-sensitive mutation E125K) target FtsL to midcell at both 28°C and 42°C (Fig. 5I and J). Introducing the D237N mutation in

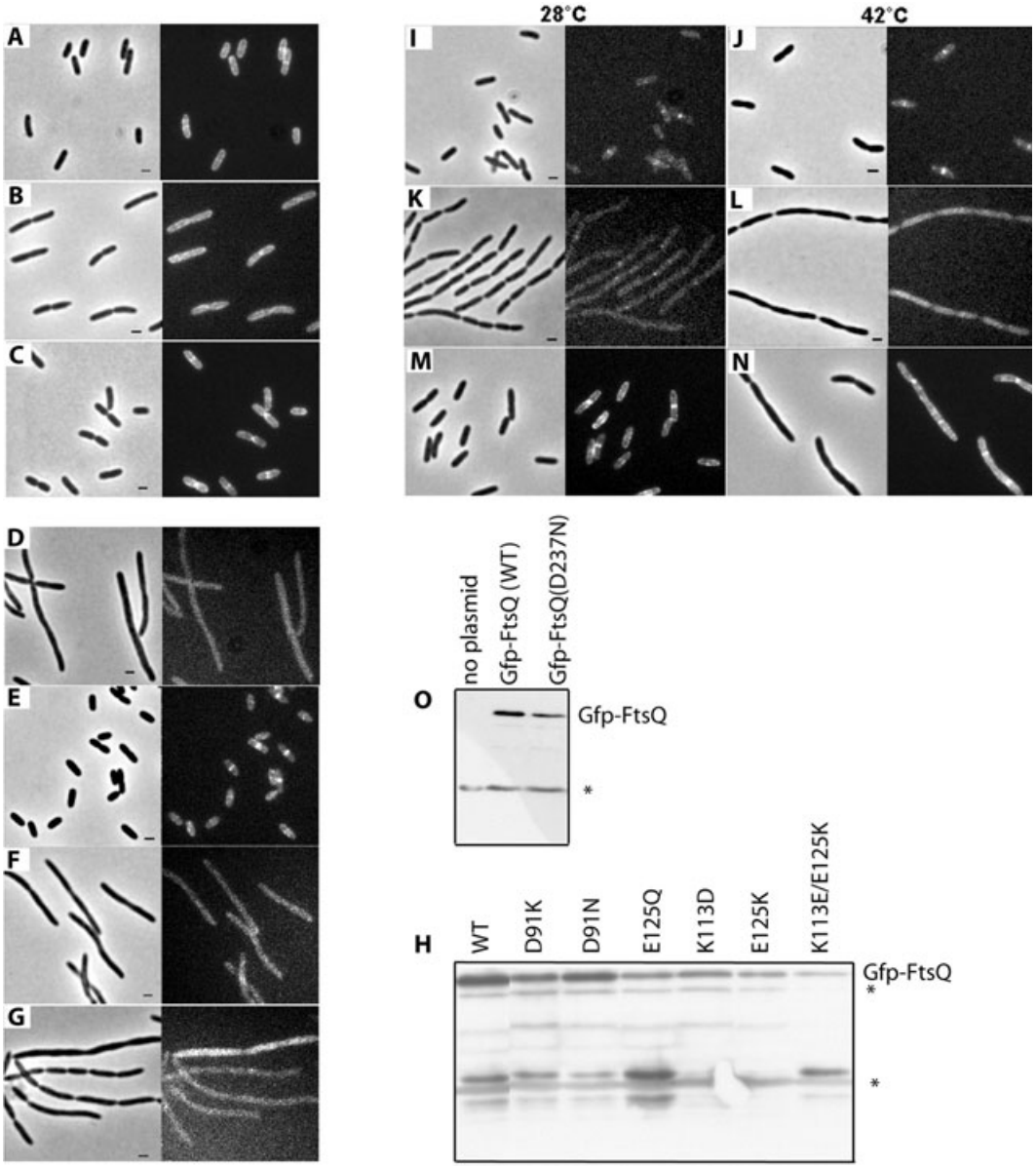

Fig. 5. Mutants affecting FtsQ localization and FtsL recruitment.
A–C. GFP–FtsQ(WT) and GFP–FtsQ(D91K) do localize, but FtsQ(K113D) does not localize to midcell.
A. pTHV039 [GFP–FtsQ(WT) (Aarsman *et al.*, 2005)].
B. pTHV056 [GFP–FtsQ(K113D].
C. pTHV053 [GFP–FtsQ(D91K)]. GFP-fusions were expressed in LMC500 at 28°C and grown to steady state in GB1.
D–G. FtsQ(K113D) complementation.
D. LMC531 [*ftsQ*1(Ts) (Taschner *et al.*, 1988)].
E. LMC531 with GFP–FtsQ(WT) shows good complementation: LMC2328 [GFP–FtsQ(WT)InCh531].
F. GFP–FtsQ(K113D) expressed from plasmid pTHV056 does not complement.
G. GFP–FtsQ(K113E-E125K) does not complement: LMC2332 [GFP–FtsQ(K113E-E125K)InCh531]. On the left, the phase contrast images and on the right, the fluorescence images are shown. The cells were grown for two mass doublings at 42°C.
H. Expression levels of the GFP fusion proteins used in FtsQ localization studies. LMC500 cells (WT) transformed with plasmids expressing GFP–FtsQ(WT) or GFP–FtsQ(mutants) were grown exponentially in TY at 28°C. Equal amounts of whole cell extract was applied to an SDS-PAGE and Immunoblotted. The blot was developed with a pAb against GFP.
I–N. Residue D237 is essential for the recruitment of FtsL but not for FtsQ localization.
I and J. LMC531 expressing FtsQ(WT) from pBadFtsQ and sYFP1-FtsL expressed from pTHV084 at 28°C and 42°C.
K and L. LMC531 expressing FtsQ(D237N) from pTHV032 (pBadftsQD237N) and sYFP1-FtsL from pTHV084.
M and N. LMC531 expressing GFP–FtsQ(D237N) from pTHV058. LMC531 was grown in GB1 to steady state at 28°C (images I, K and M) and for two mass doublings at 42°C (images J, L and N). The left images show phase contrast and right images show sYFP1 (J and L) or GFP fluorescence (N) in each example. The bar in all images is 1 μm.
O. Immunoblot developed with a polyclonal antiserum against GFP showing the expression level of GFP–FtsQ(WT) and GFP–FtsQ(D237N).

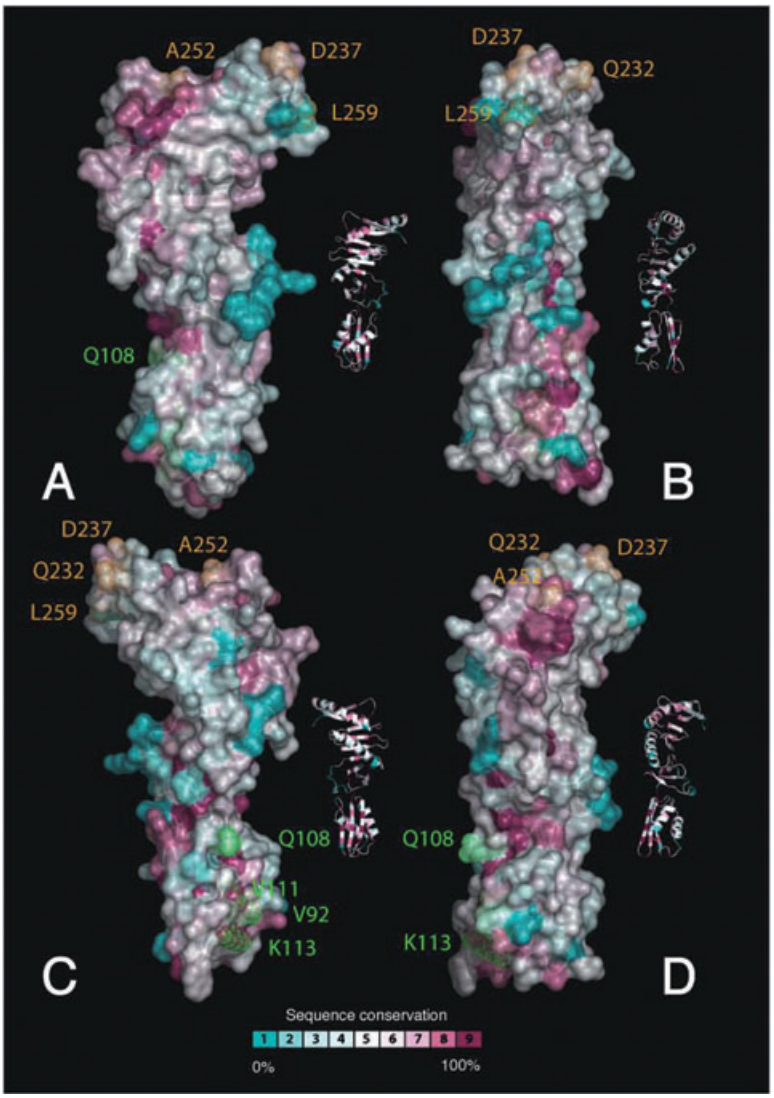

Fig. 6. Conservation plot of FtsQ. Based on an alignment of 250 different FtsQ proteins, the degree of conservation of each residue was calculated using CONSURF (Landau *et al*., 2005) and displayed on the semi-transparent surface of the structure of the *E. coli* FtsQ. The figure shows 90° rotations along the *y*-axis. The mini-ribbon plot is added to facilitate the orientation of the molecule. Sequence conservation is scored by colour [from most conserved (maroon) to most variable (blue)]. Residues depicted in orange are involved in the recruitment of FtsL/FtsB and those shown in green are implicated in FtsQ localizaton. The figure was prepared using PYMOL.

GFP–FtsQ in LMC531 cells shows a similar localization pattern as in WT FtsQ, at both temperatures (Fig. 5M and N). However, cells that carry GFP–FtsQ(D237N) no longer divide once they are shifted to the restrictive temperature (Fig. 5N). As the mutant protein itself localizes and is stable (Fig. 5O), it is reasonable to assume that the lack of cell division is caused by a failure to recruit downstream proteins to the division site. FtsL is the first protein to be recruited by FtsQ. When FtsQ(D237N) is expressed together with sYFP1-FtsL in LMC531 cells at 42°C, FtsL no longer localizes to the septum and cell division is impaired (Fig. 5L). Although FtsQ(D237N) localizes to midcell at this temperature, it is unable to form a functional complex with FtsL/FtsB and hence cell division is blocked. At 28°C, expression of sYFP1-FtsL in combination with FtsQ(D237N) in LMC531 cells shows a weak localization of sYFP1-FtsL and a chain-like growth because of a very slow division rate (Fig. 5K). Both the weak localization and the slow division rate are probably caused by competition between FtsQ(ts), FtsL and sYFP1-FtsL for FtsB. A reduction of FtsQ/L/B complexes at the division site occurs as sYFP1-FtsL cannot localize without extra FtsQ (Fig. 5I and J) and FtsQD237N is not able to recruit FtsL or FtsB. Similarly, when sCFP2-FtsB is used instead of sYFP1-FtsL, FtsQ(D237N) causes loss of normal FtsB localization, supporting the notion that FtsL and FtsB are interdependent for their localization (data not shown). In conclusion, residue D237 is essential for the localizaton of FtsL and FtsB and not for the localizaton and stability of FtsQ. From the structure, it becomes apparent that D237, which is located at the C-terminus of helix H5, is fully solvent exposed, and therefore is a good candidate for the interaction with the FtsL/FtsB complex.

This hypothesis is supported by the FtsQ mutant A252P that no longer recruits FtsL or FtsI (Goehring *et al*., 2007). A252 is solvent exposed and is located in the loop pre-

ceding the C-terminal β-strand, on the same face of FtsQ as D237 (Fig. 6).

Another mutant that failed to recruit FtsL is FtsQ65, which carries four mutations (I207F, Q232R, V244D and L259S) (Chen *et al*., 2002). Residues I207 (located in the loop leading into β-strand S10) and V244 (part of β-strand S11) are buried in the hydrophobic core between the β-sheet and helix H5. The other two mutations are solvent exposed and are close in space to D237 (Fig. 6); Q232 is one turn away from D237 and L259 is separated by G238 from D237. It is conceivable that the solvent exposed parts of these four residues, Q232, D237, A252 and L259 are involved in the recruitment of FtsL or FtsB to the division site. The importance of the C-terminal region of FtsQ for FtsL interaction is supported by previous observations where deletion mutants of FtsQ that lack the C-terminal 29 amino acids (Chen *et al*., 2002) or even the last β-strand (Goehring *et al*., 2007) fail to recruit FtsL/FtsB. Bacterial two-hybrid analyses have suggested that residues 234–277 are involved in FtsL interaction (D'Ulisse *et al*., 2007), which supports the importance of the last two β-strands of FtsQ for FtsL/FtsB interaction. Although the localization data are highly suggestive of a direct interaction between the C-terminus of FtsQ and FtsL/FtsB, they are not conclusive. It remains to be established whether a direct interaction exists between purified, full-length proteins, which would enable further characterization of site-specific mutants.

From the data presented here, it becomes clear that two functions of FtsQ, localization and recruitment, are located in separate parts of the molecule (Fig. 6). Proteins that localize FtsQ need the POTRA domain at the amino terminus of the periplasmic part of FtsQ and proteins that are recruited by FtsQ, like FtsL/FtsB, require the surface formed by the tip of the last α-helix and the two C-terminal β-strands. Both domains act together to accomplish the role of FtsQ in localizing the FtsL/FtsB complex to midcell, thereby regulating the assembly of the divisome.

Experimental procedures

Cloning, expression and purification of FtsQ

Over 50 different constructs were made that encoded the periplasmic part of FtsQ (or deletion mutants thereof) from 19 different species. Most of these proteins were His-tagged at the C-terminus, while others had a N-terminal His-tag with or without a TEV cleavage site between the tag and the protein or were fused to maltose binding protein, Thioredoxin, ZapA *Pseudomonas aeruginosa* (Low *et al*., 2004), or Ferritin from *Listeria monocyogenes*. Expression tests were done in Bl21Al cells (Invitrogen) and C41 cells (Miroux and Walker, 1996) with a 10 ml culture and purified over a Ni^{2} ± NTA spin column as described previously (van den Ent and Löwe, 2006), and expression levels were assessed on a Coomassie stained gel.

The constructs expressing the proteins that crystallized into the two structures of FtsQ described here were made as follows. The gene encoding *E. coli* FtsQ (UniProtKB/ddSwiss-Prot P06136) was amplified from genomic DNA using Pfu-Turbo (Stratagene) with a forward primer (CGATTGGcc atggATATGTCGCAGGCTGCTCTGAACACGC) and reverse primer (GGCATAActcgagTTGTTGTTCTGCCTGTGCCTG ATTTTGTTGC). The PCR product was cut with NcoI/XhoI and ligated into NcoI/XhoI digested pET28a (Novagen). This newly obtained plasmid, pFE43, was used as a template to construct ECQ6 with forward primer (CGATTGGcatatg TCAAAGCTGGTGTTGACTGGTGAACGCC) and reverse primer (GGCATAAggatccTTGTTGTTCTGCCTGTGCCTGA TTTTGTTGC), once a silent mutation was introduced to disrupt the internal NdeI site by QuickChange mutagensis (Stratagene). The insert was cleaved with BamHI/NdeI and ligated into BamHI/NdeI digested pHis17. The newly obtained plasmid, pFE48, encodes residues 58–276 of *E. coli* FtsQ followed by GSHHHHHH.

Similarly, the periplasmic part of *Y. enterocolitica* FtsQ (UniProtKB/TrEMBL A1JJJ6) was amplified using PfuTurbo from genomic DNA from ATCC (9610D) as well as forward primer (CGATTGGgctagcTCTAAACTGGTGGTGACCGGT GAGCGCC) and reverse primer (TGACTACctcgagTC ATTGTTGTTTTGCCTGTGCCTGATTC). The PCR product was cloned into XhoI/NheI digested pET28b, resulting in plasmid pFE65 that encodes the major, periplasmic part of *Y. enterocolitica* FtsQ (residues 59–285) with a N-terminal His-tag.

Constructs used for the analytical ultracentrifugation experiments were made as follows. The periplasmic parts of FtsQ from *S. aureus* (residues 249–439, plasmid pFE162), from *C. diphtheria* (residues 29–224, plasmid pFE160) and from *L. monocytogenes* (residues 53–270, plasmid pFE164) were cloned into pHis17 by restriction-free cloning (van den Ent and Löwe, 2006).

All constructs were expressed in C41 cells by inducing them with 1 mM IPTG (Miroux and Walker, 1996) at 22°C for 6 h. The protein was purified over a HisTrap HP column (GE Healthcare) at pH 8.0 as described previously (van den Ent *et al*., 2006). Once FtsQ eluted from the column, it was further purified over a size exclusion column Sephacryl S200 in 20 mM Tris, 1 mM EDTA, 1 mM Na-azide, pH 8.5 (TEN8.5) for *E. coli* FtsQ and *L. monocytogenes* FtsQ, in 20 mM Tris, 1 mM EDTA, 1 mM NaAzide, 200 mM NaCl, pH 7.0 (TEN200) for *Y. enterocolitica* FtsQ, in 20 mM Tris, 1 mM EDTA, 1 mM NaAzide, 50 mM NaCl, pH 7.0 (TEN50) for *S. aureus* FtsQ and in 20 mM Tris, 1 mM EDTA, 1 mM Na-azide, pH 7.5 (TEN7.5) for *C. diphtheria* FtsQ. Proteins were concentrated by ultrafiltration using Vivaspin 10 MWCO (Vivascience) up to a concentration of 32 mg ml^{-1} (*E. coli* FtsQ and *L. monocytogenes* FtsQ) and 10 mg ml^{-1} (remaining proteins). Selenomethionine FtsQ from *E. coli* was expressed in C41 cells over night at 22°C, essentially as described previously (van den Ent *et al*., 2006). The protein was purified as shown for the non-substituted protein, except that 5 mM β-mercaptoethanol was added to all buffers for the Ni^{2+} column and 5 mM dithiothreitol (DTT) was used in the gelfiltration buffer. Typical yields were 4.5 mg of selenomethionine substituted FtsQ per litre of culture.

Table 1. Crystallographic data.

Crystal	Wavelength(Å)	Resolution (Å)	I/σI[a]	R_m[b]	Multiplicity[c]
PEAK	0.9792	3.0	14.7(2.8)	0.078	5.4
HREM	0.8726	3.5	18.0(7.2)	0.068	5.6
ECQ	0.9392	2.7	9.9(2.3)	0.104	3.1
YEQ	0.9393	3.4	13.6(3.9)	0.072	5.3

ECQ:$P6_5$: a, 148.33 Å; b, 148.33 Å; c, 69.14 Å.
YEQ:$P6_2$: a, 160.76 Å; b, 160.76 Å; c, 54.58 Å.
a. Signal to noise ratio of intensities, highest resolution bin in brackets.
b. R_m: $S_hS_i|I(h,i) - I(h)|/S_hS_i\, I(h,i)$ where I(h,i) are symmetry-related intensities and I(h) is the mean intensity of the reflection with unique index h.
c. Multiplicity for unique reflections, for MAD datasets I(+) and I(–) are kept separate.

Escherichia coli FtsN (FtsN15, residues 243–319) was expressed and purified as described previously (Yang *et al.*, 2004).

Mutational analysis of FtsQ

In order to verify the register of the last two β-strands in FtsQ, two mutants were made introducing a selenomethionine at V254 and L246 of *E. coli* FtsQ. Mutagenesis was carried out by QuickChange (Stratagene) using the following primers: for L246M forward primer GGATTAGCTACGTTGATATGCGT TATGACTCTGGAGC and its complement and for V256M forward primer GACTCTGGAGCGGCAATGGGCTGGGC GCCC and its complement. Selenomethionine-containing protein was expressed and purified as described for the non-mutated protein and crystallized under similar conditions as the WT protein (see below).

Crystallization and structure determination

Escherichia coli FtsQ was crystallized at 8 mg ml^{-1} by sitting-drop vapour diffusion after mixing in equimolar ratio of FtsN15 [residues 243–319 (Yang *et al.*, 2004)], in 33 mM n-octyl-β-D-glucoside, 50 mM Tris pH 8.5, 8% PEG550MME, 8% PEG20K, 1.2 M NaFormate at 4°C. The crystals were flash-frozen in liquid nitrogen after increasing the PEG550MME to 18%. Crystals used for phasing were grown in 25 mM n-hexyl-B-D-glucoside, 50 mM Tris pH 8.9, 8% PEG550MME, 8% PEG20K, 0.8 M NaFormate using selenomethionine substituted *E. coli* FtsQ and FtsN15 at the same concentration as for the native proteins. The crystals were cryoprotected by increasing the PEG550MME to 15% while leaving the other components of the mother liquor at the same concentration.

Yersinia enterocolitica FtsQ crystallized at 10 mg ml^{-1} in 1.5 M $LiCl_2$, 10% PEG6000, 100 mM Bicine, pH 8.4, using sitting drop at 19°C. It was flash-frozen in liquid nitrogen in the presence of the mother liquor, supplemented with 1.9 M Naformate.

Escherichia coli FtsQ crystals belong to spacegroup $P6_5$ with two molecules in the asymetric unit. *Y. enterocolitica* FtsQ crystallized in spacegroup $P6_2$, also with two molecules in the asymmetric unit. Cell constants and crystallographic data are summarized in Table 1. Datasets were collected at European synchrotron radiation facility (ESRF) beamlines ID23-1 (*E. coli* FtsQ native and selenomethionine) and ID14-4 (*Y. enterocolitica* FtsQ).

All data were indexed and integrated with MOSFLM (Leslie, 1991) and further processed using the CCP4 package (Collaborative Computing Project, 1994). Initially, 10 selenomethionine sites were found with SHELXD (Sheldrick, 1991) using the PEAK dataset from *E. coli* FtsQ (ECQ, Table 1). The co-ordinates of these sites were imported into SHARP (de la Fortelle and Bricogne, 1997) together with the HREM dataset, six additional sites were added and phases were calculated. The model was built manually with the program MAIN (Turk, 1992) and refined using CNS (Brünger *et al.*, 1998) and Refmac (Collaborative Computing Project, 1994). The structure of *Y. enterocolitica* FtsQ was solved by molecular replacement using the model of *E. coli* FtsQ in Phaser (McCoy *et al.*, 2004). Details of the refined models are shown in Table 2.

Conservation map

The conservation map shows the relative degree of conservation among 250 sequences of FtsQ/DivIB proteins. The empirical Bayesian paradigm (Mayrose *et al.*, 2004) was used in the ConSurf Server (http://consurf.tau.ac.il/) to calculate the rate of evolution at each residue (Landau *et al.*, 2005).

Analytical ultracentrifugation

The periplasmic domains of FtsQ from *E. coli*, *Y. enterocolitica*, *S. aureus*, *C. diphtheria* and *L. monocytogenes* were subjected to sedimentation equilibrium experiments. The proteins were diluted to an OD_{280} of 0.5 and dialyzed over night in 20 mM Tris, 1 mM EDTA, 100 mM NaCl, pH 8.5 for *E. coli*, *C. diphtheria* and *L. monocytogenes* FtsQ, and in 20 mM Tris, 1 mM EDTA, 100 mM NaCl, pH 7.0 for *S. aureus* (supplemented with 1 mM DTT) and *Y. enterocolitica* FtsQ. The runs were done in a Beckman Optima XL-I analytical ultracentrifuge with Ti-50 rotor using interference and absorbance at 280 nm, at 10°C. Samples were loaded into six-sector 12 mm path length cells and spun at 20 000, 30 000 and 45 000 r.p.m. until they reach equilibrium as judged by the absence of changes in the subsequent scans. Data were analysed using UltraSpin software (http://www.mrc-cpe.cam.ac.uk).

Localization- and recruitment-defective mutants of FtsQ

Mutants D91K and K113D were obtained by double PCR. In the first PCR, a forward primer 1Fw (5′-CGGAT

Table 2. refinement statistics.

	E. coli FtsQ	*Y. enterocolitica* FtsQ
Construct modelled residues	A: 58–260; B: 58–259	A: 57–258; B: 55–258
Resolution (Å)	2.7	3.4
R-factor, R-free[a]	0.237, 0.288	0.293, 0.329
B average[b]	58.29 Å^2	151.16 Å^2
Geometry bonds/angles[c]	0.014 Å, 1.639°	0.0098 Å, 1.51°
Ramachandran[d]	85.7%/0.0%	62.6%/0.0%
PDB ID[e]	2vh1/r2vh1sf	2vh2/r2vh2sf

a. 5% of reflections were randomly selected for determination of the free R-factor, prior to any refinement.
b. Temperature factors averaged for all atoms.
c. RMS deviations from ideal geometry for bond lengths and restraint angles (Engh and Huber, 1991).
d. Percentage of residues in the 'most favoured region' of the Ramachandran plot and percentage of outliers [PROCHECK (Laskowski *et al.*, 1993)].
e. Protein Data Bank identifiers for co-ordinates and structure factors respectively.

GCtctagaGAAGATGCGCAACGCC), introducing an XbaI site, was used together with a mutant-specific reverse primer [for the D91K mutant: D91KRev (5′-GGATGATGT TAACCTTCTGGGTCATAAAGG) and for K113D: 5Rev (5′-CAGGCCACTGATCACGGACGCTCAC)] using pTHV039 (Aarsman *et al.*, 2005) as template. The resulting PCR products were forward primers in the second PCR. The D91K forward primer was used together with the reverse primer 4Rev (5′-CTTCCGCgtcgacCATATG) that introduced a SalI site. This site was used to clone the insert into pTHV004 plasmid (a pBluescript derivative) to re-establish full-length *ftsQ*. The K113D mutation was generated using the reverse primer 6Rev (5′-CTCGCATTgggcccAAGCTTTCATTGTTG TTCTGCC). This primer introduced an ApaI site, which was used to clone the PCR product into the pBluescript KS+ vector. The mutations D91N was obtained using QuickChange Site-Directed Mutagenesis (Stratagene, La Jolla) with pBADFtsQ as template and the primer QC-D91NFw (5′-GGTACCTTTATGACCCAGAATGTTAACATCATCCAGA CGC) together with its complement. For the double mutation K113E-E125K, the *ftsQ* gene with the E125K mutation was obtained from the chromosome by a PCR on LMC531 (Taschner *et al.*, 1988) using FtsQ*Eco*RIsense (CGAgaattc AACAACAACTCGCAGGCTGCTCT) as a forward primer and 6Rev (5′-CTCGCATTGGGCCCaagcttTCATTGTTGT TCTGCC) as a reverse primer. The restriction sites EcoRI and HindIII introduced during this PCR were used to ligate the PCR product into the corresponding sites of the pTHV039 (Aarsman *et al.*, 2005) vector. The resulting vector, pTHV075, was used as a template in the QuickChange Site-Directed Mutagenesis to introduce the K113E mutation, using FtsQK113EFw (5′-GGATTAAGCAGGTGAGCGTCAGAGAG CAGTGGCC TGATGAATTG) and its complement, which resulted in the pTHV076 plasmid.

The KpnI-HindIII fragments of pBluescript KS+, pTHV004 and pBADFtsQ, containing the mutated *ftsQ* genes, were ligated into the corresponding sites of pTHV039 to replace the WT *ftsQ* gene and generate GFP fusion proteins. This resulted in plasmids pTHV053, pTHV054, pTHV055 and pTHV056 expressing GFP–FtsQ(D91K), GFP–FtsQ(D91N), GFP–FtsQ(E125Q) and GFP–FtsQ(K113D) respectively. The mutation D237N was obtained, using the QuickChange Site-Directed Mutagenesis method of Stratagene with the oligonucleotides QC-D237NFw (GGTTTTACAGCAGCAGGC GCAAACaaATGGCAAACGGATTAGCTACG) and QC-D237NRev (CGTAGCTAATCCGTTTGCCATttGTTTGCGCC TGCTGCTGTAAAACC) and the pBADFtsQ plasmid as template, resulting in pTHV032. The resulting *ftsQ*(*D237N*) gene was cloned from the pBADFtsQ plasmid with the KpnI and HindIII restriction sites into the corresponding sites of the pTHV039 plasmid, creating pTHV058. pTHV039 is a derivative of pTrc99A, which contains a weakened *Trc* promoter, the *gfp-mut2* gene, and the WT *ftsQ* gene (Aarsman *et al.*, 2005).

Gfp-ftsQ genes were inserted into the *E. coli* chromosome at the λ attachement site using the λInCh method, described previously (Boyd *et al.*, 2000). The resulting strains were confirmed by PCR analysis, sequencing of the insertion and sequencing of the endogenous *ftsQ* gene.

Cloning of sYFP1-FtsL. The gene encoding FtsL was amplified from the chromosome of LMC500 (Taschner *et al.*, 1988), using FtsLEcoRIFw (5′-GCGGCGCCGCCGgaattc AACAACAACATGATCAGCAGAGTGACAGAAGC) and FtsLHindIIIRev (5′-CTCGCATTGGGCCCaagcttATTTTTGCA CTACGATATTTTCTTGTG ACGG) as primers. The PCR product coding for FtsL was digested with EcoRI and HindIII and ligated into pJP010-linkerQ that expresses sYFP1-FtsQ, which was digested with the same enzymes. This resulted in plasmid pTHV084. pJP010-linkerQ is a derivative of pTHV039 where the ampicillin resitance and ColE1 origin of replication are replaced by chloramphenicol resistance and a P15a replication origin, respectively, as described (Aarsman *et al.*, 2005). The *gfp-mut2* is replaced by *syfp1* (Kremers *et al.*, 2006). A list of constructs and strains is available in Tables S1 and S2 in the supplementary information.

Media and bacterial strains. The bacteria were grown in rich medium (TY), consisting of 50 g bactotrypton, 25 g yeast extract, 15 mMol NaOH and 0.5% NaCl, or to steady state in glucose minimal medium (GB1), containing 6.33 g K_2HPO_4 $3H_2O$, 2.95 g KH_2PO_4, 1.05 g $(NH_4)_2$ SO_4, 0.10 g $MgSO_4$ $7H_2O$, 0.28 mg $FeSO_4$ $7H_2O$, 7.1 mg $Ca(NO_3)_2$ $4H_2O$, 4 mg thiamine, 4 g glucose and 50 mg lysine per litre, pH 7.0. Where appropriate, these media were supplemented with ampicillin at 100 μg ml^{-1} or chloramphenicol at 35 μg ml^{-1} as indicated.

Acknowledgements

We would like to thank the beamlines scientists at beamlines ID14-4 and ID23-1 (ESRF) and Gert-Jan Kremers and Theodorus J.W. Gadella Jr for the gift of the plasmid pGEX-sYFP1 and psCFP2-C1, Dana Boyd for the gift of strains and plasmids needed for the λInCh integrations, Jan-Willem de Gier for the gift of pBAD18FtsQ and the polyclonal antiserum against the amino-terminus of FtsQ. Mirjam Aarsman and Reinier Boon from University of Amsterdam for technical assistance and Martine Nguyen-Distèche from the university of Liège for fruitful discussions. This work was supported in part by a vernieuwingsimpuls Grant 016.001.024 (T.d.B.) of the Netherlands Organization for Scientific Research (NWO).

References

Aarsman, M.E., Piette, A., Fraipont, C., Vinkenvleugel, T.M., Nguyen-Disteche, M., and den Blaauwen, T. (2005) Maturation of the *Escherichia coli* divisome occurs in two steps. *Mol Microbiol* **55:** 1631–1645.

Alarcon, F., Ribiero de Vasconcelos, A.T., Yim, L., and Zaha, A. (2007) Genes involved in cell division in mycoplasmas. *Genet Mol Biol* **30:** 174–181.

Bernhardt, T.G., and de Boer, P.A. (2003) The *Escherichia coli* amidase AmiC is a periplasmic septal ring component exported via the twin-arginine transport pathway. *Mol Microbiol* **48:** 1171–1182.

Bernhardt, T.G., and de Boer, P.A.J. (2004) Screening for synthetic lethal mutants in *Escherichia coli* and identification of EnvC (YibP) as a periplasmic septal ring factor with murein hydrolase activity. *Mol Microbiol* **52:** 1255–1269.

Bertsche, U., Kast, T., Wolf, B., Fraipont, C., Aarsman, M.E., Kannenberg, K., *et al.* (2006) Interaction between two murein (peptidoglycan) synthases, PBP3 and PBP1B, in *Escherichia coli*. *Mol Microbiol* **61:** 675–690.

de Boer, P., Crossley, R., and Rothfield, L. (1992) The essential bacterial cell-division protein FtsZ Is a Gtpase. *Nature* **359:** 254–256.

Boyd, D., Weiss, D.S., Chen, J.C., and Beckwith, J. (2000) Towards single-copy gene expression systems making gene cloning physiologically relevant: lambda InCh, a simple *Escherichia coli* plasmid-chromosome shuttle system. *J Bacteriol* **182:** 842–847.

Brünger, A., Adams, P.D., Clore, G.M., DeLano, W.L., Gros, P., Grosse-Kunstleve, R.W., *et al.* (1998) Crystallography & NMR system: a new software suite for macromolecular structure determination. *Acta Crystallogr Section D-Biolog Crystallogr* **54:** 905–921.

Buddelmeijer, N., and Beckwith, J. (2004) A complex of the *Escherichia coli* cell division proteins FtsL, FtsB and FtsQ forms independently of its localization to the septal region. *Mol Microbiol* **52:** 1315–1327.

Buddelmeijer, N., Aarsman, M.E.G., Kolk, A.H.J., Vicente, M., and Nanninga, N. (1998) Localization of cell division protein FtsQ by immunofluorescence microscopy in dividing and nondividing cells of *Escherichia coli*. *J Bacteriology* **180:** 6107–6116.

Carson, M.J., Barondess, J., and Beckwith, J. (1991) The FtsQ protein of *Escherichia coli*: membrane topology, abundance, and cell division phenotypes due to overproduction and insertion mutations. *J Bacteriol* **173:** 2187–2195.

Chen, J.C., and Beckwith, J. (2001) FtsQ, FtsL and FtsI require FtsK, but not FtsN, for co- localization with FtsZ during *Escherichia coli* cell division. *Mol Microbiol* **42:** 395–413.

Chen, J.C., Weiss, D.S., Ghigo, J.M., and Beckwith, J. (1999) Septal localization of FtsQ, an essential cell division protein in *Escherichia coli*. *J Bacteriol* **181:** 521–530.

Chen, J.C., Minev, M., and Beckwith, J. (2002) Analysis of *ftsQ* mutant alleles in *Escherichia coli*: complementation, septal localization, and recruitment of downstream cell division proteins. *J Bacteriol* **184:** 695–705.

Collaborative Computing Project, N. (1994) The CCP4 Suite: programs for protein crystallography. *Acta Crystallogr D* **50:** 760–763.

D'Ulisse, V., Fagioli, M., Ghelardini, P., and Paolozzi, L. (2007) Three functional subdomains of the *Escherichia coli* FtsQ protein are involved in its interaction with the other division proteins. *Microbiology* **153:** 124–138.

Dai, K., Xu, Y.F., and Lutkenhaus, J. (1993) Cloning and characterization of FtsN, an essential cell-division gene in *Escherichia Coli* isolated as a multicopy suppressor of Ftsa12(ts). *J Bacteriology* **175:** 3790–3797.

Daniel, R.A., and Errington, J. (2000) Intrinsic instability of the essential cell division protein FtsL of *Bacillus subtilis* and a role for DivIB protein in FtsL turnover. *Mol Microbiol* **36:** 278–289.

Di Lallo, G., Fagioli, M., Barionovi, D., Ghelardini, P., and Paolozzi, L. (2003) Use of a two-hybrid assay to study the assembly of a complex multicomponent protein machinery: bacterial septosome differentiation. *Microbiology* **149:** 3353–3359.

Engh, R.A., and Huber, R. (1991) Accurate bond and angle parameters for x-ray protein-structure refinement. *Acta Crystallogr Section A* **47:** 392–400.

van den Ent, F., and Löwe, J. (2006) RF cloning: a restriction-free method for inserting target genes into plasmids. *J Biochem Biophys Methods* **67:** 67–74.

van den Ent, F., Leaver, M., Bendezu, F., Errington, J., de Boer, P., and Löwe, J. (2006) Dimeric structure of the cell shape protein MreC and its functional implications. *Mol Microbiol* **62:** 1631–1642.

Erickson, H.P. (1995) FtsZ, a prokaryotic homolog of tubulin? *Cell* **80:** 367–370.

Erickson, H.P., Taylor, D.W., Taylor, K.A., and Bramhill, D. (1996) Bacterial cell division protein FtsZ assembles into protofilament sheets and minirings, structural homologs of tubulin polymers. *Proc Natl Acad Sci USA* **93:** 519–523.

Errington, J., Daniel, R.A., and Scheffers, D.J. (2003) Cytokinesis in bacteria. *Microbiol Mol Biol Rev* **67:** 52–65.

de la Fortelle, E., and Bricogne, G. (1997) Maximum-likelihood heavy-atom parameter refinement for multiple isomorphous replacement and multiwavelength anomalous diffraction methods. *Macromolr Crystallogr* **276**: pp. 472–494

Gerding, M.A., Ogata, Y., Pecora, N.D., Niki, H., and de Boer, P.A. (2007) The *trans*-envelope Tol–Pal complex is part of the cell division machinery and required for proper outer-

membrane invagination during cell constriction in *E. coli*. *Mol Microbiol* **63:** 1008–1025.
Goehring, N.W., and Beckwith, J. (2005) Diverse paths to midcell: assembly of the bacterial cell division machinery. *Curr Biol* **15:** R514–R526.
Goehring, N.W., Gueiros-Filho, F., and Beckwith, J. (2005) Premature targeting of a cell division protein to midcell allows dissection of divisome assembly in *Escherichia coli*. *Genes Dev* **19:** 127–137.
Goehring, N.W., Gonzalez, M.D., and Beckwith, J. (2006) Premature targeting of cell division proteins to midcell reveals hierarchies of protein interactions involved in divisome assembly. *Mol Microbiol* **61:** 33–45.
Goehring, N.W., Petrovska, I., Boyd, D., and Beckwith, J. (2007) Mutants, suppressors, and wrinkled colonies: mutant alleles of the cell division gene *ftsQ* point to functional domains in FtsQ and a role for domain 1C of FtsA in divisome assembly. *J Bacteriol* **189:** 633–645.
Guzman, L.M., Weiss, D.S., and Beckwith, J. (1997) Domain-swapping analysis of FtsI, FtsL, and FtsQ, bitopic membrane proteins essential for cell division in *Escherichia coli*. *J Bacteriol* **179:** 5094–5103.
Harrison, S.C. (1996) Peptide–surface association: the case of PDZ and PTB domains. *Cell* **86:** 341–343.
Holm, L., and Sander, C. (1993) Protein-structure comparison by alignment of distance matrices. *J Mol Biol* **233:** 123–138.
Karimova, G., Dautin, N., and Ladant, D. (2005) Interaction network among *Escherichia coli* membrane proteins involved in cell division as revealed by bacterial two-hybrid analysis. *J Bacteriol* **187:** 2233–2243.
Katis, V.L., and Wake, R.G. (1999) Membrane-bound division proteins DivIB and DivIC of *Bacillus subtilis* function solely through their external domains in both vegetative and sporulation division. *J Bacteriol* **181:** 2710–2718.
Kim, S., Malinverni, J.C., Sliz, P., Silhavy, T.J., Harrison, S.C., and Kahne, D. (2007) Structure and function of an essential component of the outer membrane protein assembly machine. *Science* **317:** 961–964.
Kremers, G.J., Goedhart, J., van Munster, E.B., and Gadella, T.W., Jr (2006) Cyan and yellow super fluorescent proteins with improved brightness, protein folding, and FRET Forster radius. *Biochemistry* **45:** 6570–6580.
Landau, M., Mayrose, I., Rosenberg, Y., Glaser, F., Martz, E., Pupko, T., and Ben-Tal, N. (2005) ConSurf 2005: the projection of evolutionary conservation scores of residues on protein structures. *Nucleic Acids Res* **33:** W299–W302.
Laskowski, R.A., MacArthur, M.W., Moss, D.S., and Thornton, J.M. (1993) Procheck – a program to check the stereochemical quality of protein structures. *J Appl Crystallogr* **26:** 283–291.
Leslie, A.G.W. (1991) *Recent Changes to the MOSFLM Package for Processing Film and Image Plate Data*. Daresbury: SERC Laboratory.
Low, H.H., Moncrieffe, M.C., and Löwe, J. (2004) The crystal structure of ZapA and its modulation of FtsZ polymerisation. *J Mol Biol* **341:** 839–852.
Löwe, J., and Amos, L.A. (1998) Crystal structure of the bacterial cell-division protein FtsZ. *Nature* **391:** 203–206.
Löwe, J., and Amos, L.A. (1999) Tubulin-like protofilaments in Ca2+-induced FtsZ sheets. *EMBO J* **18:** 2364–2371.
Lu, C.L., Reedy, M., and Erickson, H.P. (2000) Straight and curved conformations of FtsZ are regulated by GTP hydrolysis. *J Bacteriol* **182:** 164–170.
McCoy, A.J., Storoni, L.C., and Read, R.J. (2004) Simple algorithm for a maximum-likelihood SAD function. *Acta Crystallogr D Biol Crystallogr* **60:** 1220–1228.
Mayrose, I., Graur, D., Ben-Tal, N., and Pupko, T. (2004) Comparison of site-specific rate-inference methods for protein sequences: empirical Bayesian methods are superior. *Mol Biol Evol* **21:** 1781–1791.
Mengin-Lecreulx, D., van Heijenoort, J., and Park, J.T. (1996) Identification of the mpl gene encoding UDP-N-acetylmuramate: 1-alanyl-gamma-D-glutamyl-meso-diaminopimelate ligase in *Escherichia coli* and its role in recycling of cell wall peptidoglycan. *J Bacteriol* **178:** 5347–5352.
Miroux, B., and Walker, J.E. (1996) Over-production of proteins in *Escherichia coli*: mutant hosts that allow synthesis of some membrane proteins and globular proteins at high levels. *J Mol Biol* **260:** 289–298.
Mukherjee, A., and Lutkenhaus, J. (1994) Guanine nucleotide-dependent assembly of FtsZ into filaments. *J Bacteriol* **176:** 2754–2758.
Mukherjee, A., Dai, K., and Lutkenhaus, J. (1993) *Escherichia coli* cell division protein FtsZ is a guanine nucleotide binding protein. *Proc Natl Acad Sci USA* **90:** 1053–1057.
Pichoff, S., and Lutkenhaus, J. (2002) Unique and overlapping roles for ZipA and FtsA in septal ring assembly in *Escherichia coli*. *EMBO J* **21:** 685–693.
Pichoff, S., and Lutkenhaus, J. (2005) Tethering the Z ring to the membrane through a conserved membrane targeting sequence in FtsA. *Mol Microbiol* **55:** 1722–1734.
Piette, A., Fraipont, C., Den Blaauwen, T., Aarsman, M.E., Pastoret, S., and Nguyen-Disteche, M. (2004) Structural determinants required to target penicillin-binding protein 3 to the septum of *Escherichia coli*. *J Bacteriol* **186:** 6110–6117.
RayChaudhuri, D., and Park, J.T. (1992) *Escherichia coli* cell-division gene *ftsZ* encodes a novel GTP-binding protein. *Nature* **359:** 251–254.
Robinson, A.C., Kenan, D.J., Hatfull, G.F., Sullivan, N.F., Spiegelberg, R., and Donachie, W.D. (1984) DNA sequence and transcriptional organization of essential cell division genes *ftsQ* and *ftsA* of *Escherichia coli*: evidence for overlapping transcriptional units. *J Bacteriol* **160:** 546–555.
Robson, S.A., and King, G.F. (2006) Domain architecture and structure of the bacterial cell division protein DivIB. *Proc Natl Acad Sci USA* **103:** 6700–6705.
Rowland, S.L., Katis, V.L., Partridge, S.R., and Wake, R.G. (1997) DivIB, FtsZ and cell division in *Bacillus subtilis*. *Mol Microbiol* **23:** 295–302.
Sánchez-Pulido, L., Devos, D., Genevrois, S., Vicente, M., and Valencia, A. (2003) POTRA: a conserved domain in the FtsQ family and a class of beta-barrel outer membrane proteins. *Trends Biochem Sci* **28:** 523–526.
Sheldrick, G.M. (1991) Heavy atom location using SHELXS-90. Daresbury CCP4 Meeting.

Taschner, P.E.M., Huls, P.G., Pas, E., and Woldringh, C.L. (1988) Division behavior and shape changes in isogenic Ftsz, Ftsq, Ftsa, Pbpb, and Ftse cell-division mutants of *Escherichia Coli* during temperature shift experiments. *J Bacteriol* **170:** 1533–1540.

Turk, D. (1992) Weiterentwicklung eines Programms für Molekülgrafik und Elektrondichte-Manipulation und seine Anwendung auf verschiedene Protein-Strukturaufklärungen. PhD Thesis, Technische Universität München.

Vicente, M., and Rico, A.I. (2006) The order of the ring: assembly of *Escherichia coli* cell division components. *Mol Microbiol* **61:** 5–8.

Weiss, D.S., Chen, J.C., Ghigo, J.M., Boyd, D., and Beckwith, J. (1999) Localization of FtsI (PBP3) to the septal ring requires its membrane anchor, the Z ring, FtsA, FtsQ, and FtsL. *J Bacteriology* **181:** 508–520.

Yang, J.C., van den Ent, F., Neuhaus, D., Brevier, J., and Lowe, J. (2004) Solution structure and domain architecture of the divisome protein FtsN. *Mol Microbiol* **52:** 651–660.

Yu, X.C., and Margolin, W. (1997) Ca2+-mediated GTP-dependent dynamic assembly of bacterial cell division protein FtsZ into asters and polymer networks *in vitro*. *EMBO J* **16:** 5455–5463.

